

Washington University School of Medicine

Digital Commons@Becker

2020-Current year OA Pubs

Open Access Publications

5-1-2021

The poly(ADP-ribosyl)ation of BRD4 mediated by PARP1 promoted pathological cardiac hypertrophy

Zhenzhen Li
Sun Yat-sen University

Zhen Guo
Washington University School of Medicine in St. Louis

Rui Lan
Sun Yat-sen University

Sidong Cai
Sun Yat-sen University

Zhirong Lin
Sun Yat-sen University

See next page for additional authors

Follow this and additional works at: https://digitalcommons.wustl.edu/oa_4

Recommended Citation

Li, Zhenzhen; Guo, Zhen; Lan, Rui; Cai, Sidong; Lin, Zhirong; Li, Jingyan; Wang, Junjian; Li, Zhuoming; and Liu, Peiqing, "The poly(ADP-ribosyl)ation of BRD4 mediated by PARP1 promoted pathological cardiac hypertrophy." *Acta Pharmaceutica Sinica B*. 11, 5. 1286 - 1299. (2021).
https://digitalcommons.wustl.edu/oa_4/288

This Open Access Publication is brought to you for free and open access by the Open Access Publications at Digital Commons@Becker. It has been accepted for inclusion in 2020-Current year OA Pubs by an authorized administrator of Digital Commons@Becker. For more information, please contact vanam@wustl.edu.

Authors

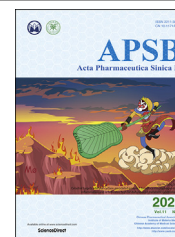
Zhenzhen Li, Zhen Guo, Rui Lan, Sidong Cai, Zhirong Lin, Jingyan Li, Junjian Wang, Zhuoming Li, and Peiqing Liu



Chinese Pharmaceutical Association
Institute of Materia Medica, Chinese Academy of Medical Sciences

Acta Pharmaceutica Sinica B

www.elsevier.com/locate/apsb
www.sciencedirect.com



ORIGINAL ARTICLE

The poly(ADP-ribosylation) of BRD4 mediated by PARP1 promoted pathological cardiac hypertrophy



Zhenzhen Li^a, Zhen Guo^{a,b}, Rui Lan^a, Sidong Cai^a, Zhirong Lin^a,
Jingyan Li^c, Junjian Wang^a, Zhuoming Li^{a,*}, Peiqing Liu^{a,*}

^aDepartment of Pharmacology and Toxicology, School of Pharmaceutical Sciences, National and Local United Engineering Lab of Druggability and New Drugs Evaluation, Guangdong Engineering Laboratory of Druggability and New Drug Evaluation, Guangdong Provincial Key Laboratory of New Drug Design and Evaluation, Sun Yat-sen University, Guangzhou 510006, China

^bCenter for Cardiovascular Research and Division of Cardiology, Washington University School of Medicine, St. Louis, MO 63101, USA

^cInternational Institute for Translational Chinese Medicine, School of Pharmaceutical Sciences, Guangzhou University of Chinese Medicine, Guangzhou 510006, China

Received 14 June 2020; received in revised form 18 August 2020; accepted 13 October 2020

KEY WORDS

BRD4;
PARP1;
PARylation;
Isoproterenol;
Cardiac hypertrophy;
RNA Pol II;

Abstract The bromodomain and extraterminal (BET) family member BRD4 is pivotal in the pathogenesis of cardiac hypertrophy. BRD4 induces hypertrophic gene expression by binding to the acetylated chromatin, facilitating the phosphorylation of RNA polymerases II (Pol II) and leading to transcription elongation. The present study identified a novel post-translational modification of BRD4: poly(ADP-ribosylation) (PARylation), that was mediated by poly(ADP-ribose)polymerase-1 (PARP1) in cardiac hypertrophy. BRD4 silencing or BET inhibitors JQ1 and MS417 prevented cardiac hypertrophic responses induced by isoproterenol (ISO), whereas overexpression of BRD4 promoted cardiac hypertrophy,

Abbreviations: ANP, atrial natriuretic peptide; BET, bromodomain and extraterminal domain; BNP, brain natriuretic polypeptide; BW, body weight; CDK9, cyclin-dependent kinase 9; co-IP, co-immunoprecipitation; EF, ejection fraction; FBS, fetal bovine serum; FS, fractional shortening; HATs, histone acetyltransferases; HDACs, histone deacetylases; HE, hematoxylin-eosin; HW, heart weight; IF, immunofluorescence; ISO, isoproterenol; LVAW, left ventricular anterior wall thickness; LVID, left ventricular internal diameter; LVPW, left ventricular posterior wall thickness; NC, negative control; NRCMs, neonatal rat cardiomyocytes; NS, normal saline; PARP1, poly(ADP-ribose)polymerase-1; PBS, phosphate buffer solution; PSR, picrosirius red; RNA Pol II, RNA polymerases II; SD, Sprague–Dawley; siRNA, small-interfering RNA; TL, tibia length; TSS, transcription start sites; WGA, wheat germ agglutinin; β -AR, β -adrenergic receptor; β -MHC, β -myosin heavy chain.

*Corresponding authors. Fax: +86 20 39943026.

E-mail addresses: lizhm5@mail.sysu.edu.cn (Zhuoming Li), liuq@mail.sysu.edu.cn (Peiqing Liu).

Peer review under responsibility of Chinese Pharmaceutical Association and Institute of Materia Medica, Chinese Academy of Medical Sciences.

<https://doi.org/10.1016/j.apsb.2020.12.012>

2211-3835 © 2021 Chinese Pharmaceutical Association and Institute of Materia Medica, Chinese Academy of Medical Sciences. Production and hosting by Elsevier B.V. This is an open access article under the CC BY-NC-ND license (<http://creativecommons.org/licenses/by-nc-nd/4.0/>).

Transcription activation;
Hypertrophic genes

confirming the critical role of BRD4 in pathological cardiac hypertrophy. PARP1 was activated in ISO-induced cardiac hypertrophy and facilitated the development of cardiac hypertrophy. BRD4 was involved in the prohypertrophic effect of PARP1, as implied by the observations that BRD4 inhibition or silencing reversed PARP1-induced hypertrophic responses, and that BRD4 overexpression suppressed the anti-hypertrophic effect of PARP1 inhibitors. Interactions of BRD4 and PARP1 were observed by co-immunoprecipitation and immunofluorescence. PARylation of BRD4 induced by PARP1 was investigated by PARylation assays. In response to hypertrophic stimuli like ISO, PARylation level of BRD4 was elevated, along with enhanced interactions between BRD4 and PARP1. By investigating the PARylation of truncation mutants of BRD4, the C-terminal domain (CTD) was identified as the PARylation modification sites of BRD4. PARylation of BRD4 facilitated its binding to the transcription start sites (TSS) of hypertrophic genes, resulting in enhanced phosphorylation of RNA Pol II and transcription activation of hypertrophic genes. The present findings suggest that strategies targeting inhibition of PARP1-BRD4 might have therapeutic potential for pathological cardiac hypertrophy.

© 2021 Chinese Pharmaceutical Association and Institute of Materia Medica, Chinese Academy of Medical Sciences. Production and hosting by Elsevier B.V. This is an open access article under the CC BY-NC-ND license (<http://creativecommons.org/licenses/by-nc-nd/4.0/>).

1. Introduction

Pathological cardiac hypertrophy is an adaptive response to stress stimulation or disease, which contributes to cardiac contractile dysfunction and heart failure^{1–3}. Its typical characteristics are increased cardiomyocyte size, higher organization of sarcomere, enhanced protein synthesis and reprogramming of fetal genes, such as atrial natriuretic peptide (ANP), brain natriuretic peptide (BNP), and β -myosin heavy chain (β -MHC)². The regulatory networks governing cardiac hypertrophy are under intense investigation. Epigenetic modifications are important contributors to this process. Among them, histone acetylation is known to be crucial in cardiac physiology and pathophysiology^{4–6}, which involves three classes of regulators, including “writers” or histone acetyltransferases (HATs), “erasers” or histone deacetylases (HDACs) and “readers” or acetyl lysine binders⁷. Accumulating evidences have revealed HDACs and HATs as positive and negative regulators in pathological cardiac hypertrophy^{8–11}. Recently, the contribution of “readers” in cardiac hypertrophy attracts mounting attention.

Bromodomain and extraterminal (BET) family proteins are regarded as an important type of lysine acetylation “readers”. Since their bromodomains are responsible for binding to acetylated lysine residues in histones, they serve as chromatin-targeting modules that decipher the histone acetylation code^{12–14}. BET proteins have attracted accumulating attentions for their participation in the pathogenesis of cardiac diseases. The recent development of potent, specific and reversible BET inhibitors, like the small molecule JQ1, which competes and displaces bromodomains from acetylated chromatin, has been implicated in suppressing innate inflammatory and transcriptional networks in heart failure^{15–17}. BET family contains four subtypes, including BRD2, BRD3, BRD4 and BRDT, among which, BRD4 has been shown as a nodal regulator of the transcriptional program in cardiac hypertrophy^{18,19}. Prohypertrophic stimuli facilitates the recruitment of BRD4 to the promoter regions of target genes, and then induces the cyclin-dependent kinase 9 (CDK9)-mediated phosphorylation of RNA polymerase II (RNA Pol II) at serine 2 (Ser2), finally leading to increased transcriptional elongation of hypertrophic genes^{19,20}.

Interestingly, studies in our laboratory demonstrated an interaction between BRD4 and poly(ADP-ribose) polymerase 1

(PARP1) in cardiac hypertrophy, as implied by the co-immunoprecipitation (co-IP) and immunofluorescence (IF) results. PARP1, a member of PARP enzyme family, can modulate diverse biological processes through covalent transfer of ADP-ribose from NAD⁺ onto substrate proteins or DNA chain, known as poly(ADP-ribose)ylation (PARylation)^{21–23}. Our previous studies have revealed that PARP1 is activated and PARylates FOXO3, STAT3 and HMGB1 in cardiac hypertrophy, whereas inhibition of PARP1 by 3-aminobenzamide (3AB) and veliparib (ABT-888) prevents the development of cardiac hypertrophy^{24–27}. The observations of BRD4/PARP1 interaction thus prompt our hypothesis that BRD4 might act as a substrate protein of PARP1, and that PARylation of BRD4 by PARP1 might facilitate the recruitment of BRD4 to hyper-acetylated chromatin and enhance RNA Pol II phosphorylation, ultimately promoting transcription activation of hypertrophic biomarkers. The present study attempted to provide mechanistic insights into the interaction of BRD4 and PARP1 in pathological cardiac hypertrophy.

2. Materials and methods

2.1. Primary culture of neonatal rat cardiomyocytes (NRCMS)

Primary culture of NRCMs, isolated from the hearts of Sprague–Dawley (SD) rats (1- to 3-day-old) obtained from the Experimental Animal Center of Sun Yat-sen University, was performed as described previously²⁸. NRCMs were isolated and seeded onto six well plates at a density of 1×10^6 cells and cultured in DEME (Gibco, BRL Co., Ltd., USA) supplemented with 10% fetal bovine serum (FBS) and 0.1 mmol/L 5-bromodeoxyuridine at 37 °C with 5% CO₂. Finally, ISO (Sigma–Aldrich, St. Louis, MO, USA) was added to medium at a concentration of 10 μ mol/L and the cells were further incubated for indicated time.

2.2. Animal model, echocardiography and morphometric measurements

The animal experiments were approved by the Research Ethics Committee of Sun Yat-sen University, and were conducted under the Guide for the Care and Use of Laboratory Animals (NIH

Publications No. 8023, revised 1978). SD rats (male, 180–220 g, SPF grade, certification Nos. 44007200054721 and 1100112011043685) from the Experimental Animal Center of Guangzhou University of Chinese Medicine (Guangzhou, China) and Charles River (Beijing, China), respectively, were housed under controlled environmental conditions (a 12-h:12-h light/dark cycle and a room temperature of 21–23 °C) and had free access to standard laboratory food and water. ISO (1.2 mg/kg/day) was subcutaneously (s.c.) injected for seven consecutive days to induce cardiac hypertrophy. The vehicle control group was given equal treatments of normal saline (NS). Two-dimensional guide M-mode echocardiography was conducted with a Technos MPX ultrasound system (ESAOTE, SpAESAOTE SppA, Italy)²⁹. After that, the rats were sacrificed and then their hearts were quickly removed, weighed and then used for other measurements.

2.3. Intramyocardial delivery of adeno-associated virus

SD rats were randomized divided into two groups and anaesthetized with sodium pentobarbital (30 mg/kg, i.p.). Fentanyl (0.16 mg/kg, s.c.) was given as an analgesic agent and then rats were endotracheally intubated noninvasively connecting to respiratory machine. Open thoraces at the left fourth intercostal space to expose the heart. Then 200 µL of adeno-associated virus (10¹² particles) were injected into five to six sites along the left ventricular walls directly by a curved 25-gauge needle²¹. After the operation, thoraces and incision were sutured, and gentamicin was given to prevent infection. Adeno-associated virus expressing the si-RNA sequence of BRD4 (AAV-si-BRD4) was constructed by Hanbio Biotechnology (Shanghai, China).

2.4. Morphological and histology analysis

Hearts from animals were excised, washed in 10% potassium chloride solution and fixed with 4% paraformaldehyde. Then the hearts were embedded in paraffin and cut transversely into 5 µm sections. Serial sections were stained with hematoxylin-eosin (HE) or wheat germ agglutinin (WGA) staining to measure myocyte cross sectional areas and Picrosirius red (PSR) staining to detect collagen content.

2.5. Western blot assay and co-immunoprecipitation (co-IP) analysis

Western blot assays were performed as previously reported³⁰. For Western blotting, primary antibodies against BRD4 (Cat#128874; rabbit, diluted 1:1000), PARP1 (Cat#9532S; rabbit, diluted 1:1000), RNA Pol II (Cat#2629; mouse, diluted 1:1000) was purchased from Cell signaling Technology. RNA Pol II phosphorylation on serine 2 (Cat# ab193468; rabbit, diluted 1:5000) was bought from Abcam, ANP (Cat# PAA225Ra02; rabbit, diluted 1:1000) was purchased from Cloud-Clone Corp., PAR (Cat#: 4335-MC-100-AC; mouse, diluted 1:1000) was purchased from Trevigen (Gaithersburg, MD, USA). The signals of protein level were visualized by Image Quant LAS 4000 mini produced by GE healthcare (Waukesha, WI, USA). The intensities of the blots were quantified by the Quantity One (Bio-Rad) software. α -Tubulin was used as an internal control for total proteins.

For co-IP, anti-BRD4 (rabbit diluted 1:100) antibody and anti-PARP1 (rabbit, diluted 1:10) antibody. The IP lysates (400 µg) were incubated with the corresponding primary antibodies

overnight (rabbit normal IgG was served as control), and were incubated with protein G-agarose beads (Pierce, Rockford, IL, USA) at 4 °C for 4 h. The immunoprecipitated proteins were observed by Western blot analysis.

2.6. Quantitative real-time polymerase chain reaction (qRT-PCR)

Total RNA from heart tissues or cultured cells was extracted using Trizol reagent (Invitrogen, Carlsbad, CA, USA). The RNA extract was reversely transcribed to cDNA by the One-step RT Kit (Thermo Fisher Scientific, USA). The mRNA levels of each targeted genes were determined by using SYBR-Green Quantitative PCR kit (TOYOBO, Japan) in iCycler iQ system (Bio-Rad, USA). The amplification conditions were as follow: 15 min at 95 °C, followed by 40 cycles of 30 s at 95 °C, 1 min at 55 °C and 30 s at 72 °C. All PCR assays were done in triplicate. Rat-specific primers were synthesized by Sangon (Shanghai, China; Supporting Information Table S1). β -Actin was used as an endogenous control.

2.7. RNA interference, plasmid transfection

Three different duplex siRNAs for BRD4 (si-01, si-02, and si-03), PARP1 and negative control (NC) siRNA were purchased from GenePharma (Shanghai, China). The sequences were listed in Supporting Information Table S2. RNA interference was performed using Lipofectamine 2000 (Invitrogen, Carlsbad, CA, USA) according to the manufacturer's instructions. Western blot was conducted to determine the silencing efficiency. Given that the target effect of the siRNAs, endogenous BRD4 was knocked down using the si-421 (Supporting Information Fig. S1).

The BRD4 and Flag-PARP1 plasmids were bought from Genechem (Shanghai, China). Three large deletion BRD4 mutants (P1, P2 and P3) were constructed by inserting into the eukaryotic expressing vector GV219 with HA-tag (P1, 1–500 amino acids; P2, 501–699 amino acids; P3, 700–1400 amino acids). Cardiomyocytes were transfected with the plasmids. After treatment for 48 h, the cells were stimulated with or without ISO for 12 h.

2.8. ChIP qPCR

Chromatin was crosslinked in 1% formaldehyde for 10 min. The cross-linking reaction was stopped with glycine for 5 min. Then the cells were washed with ice cold paraformaldehyde in phosphate (PBS), harvested in PBS with protease and phosphatase inhibitors, frozen in liquid nitrogen and stored at –80 °C until processed. NRCMs were resuspended in Farnham lysis buffer (5 mmol/L PIPES, 85 mmol/L KCl, 0.5% NP40, Roche protease inhibitor cocktail) with phosphatase inhibitors and then centrifugated at 2000 rpm for 5 min at 4 °C. After centrifugation, pellets were resuspended in RIPA buffer (1×PBS, 1% NP40, 0.5% sodium deoxycholate, 0.1% SDS, Roche protease inhibitor cocktail) with protease inhibitors and transferred to microfuge tubes for sonication by a Sonics VibraCell sonicator (Covaris, USA). After sonication, sheared chromatin was collected in supernatant by centrifugation at 14,000 rpm for 15 min at 4 °C. Cleared chromatin was then immunoprecipitated with 5 µg of antibody BRD4 (Bethyl, A301-985A) attached to protein G Dynabeads (Invitrogen, USA). Following overnight IP, beads were washed five times and DNA was eluted in TE buffer (10 mmol/L Tris HCl, 0.1 mmol/L Na₂EDTA) at 65 °C for 15 min. Following reversal of crosslinks, RNase and proteinase treatment, DNA was purified

using the PCR Purification Kit (Thermo Fisher Scientific, Rockford, IL, USA) according to the protocol and used for qPCR investigation. Rat-specific primers were synthesized by Sangon (Supporting Information Table S3).

2.9. Measurement of cell surface area

NRCMs grown in 48-well plates were fixed with 4% paraformaldehyde in PBS for 15 min at room temperature, and further incubated with 0.3% TritonX-100 for 10 min, and then incubated with 0.1% rhodamine-phalloidin (Invitrogen, Carlsbad, CA, USA) for 1 h. After washing with PBS, the cells were incubated with DAPI (Cell Signaling Technology, USA). The cell surface area from randomly selected field fields (50 for each group) was measured using the built-in image analysis software.

2.10. Immunofluorescence (IF) assay

NRCMs seeded on coverslips were fixed with 4% paraformaldehyde for 30 min. After washing with PBS for three times,

the cells were permeabilized with 0.3% Triton X-100 for 10 min and followed by incubation with blocking solution at room temperature for 1 h. The cells were further treated with primary antibodies against BRD4 (diluted 1:50), and PARP1 (diluted 1:50) overnight at 4 °C, and then incubated with Alexa Fluor-labeled secondary antibody (diluted 1:100, Proteintech Group, USA). The coverslips were mounted with DAPI were detected by a confocal microscope (Zeiss, Germany).

2.11. Data and statistical analysis

The data and statistical analysis in this study comply with the recommendations on experimental design and analysis in pharmacology³¹. The data were presented as mean \pm standard error of mean (SEM). Statistical analyses between two groups were performed by unpaired Student's *t*-test. Differences among multiple groups were tested by one-way ANOVA with Bonferroni *post hoc* test. In all cases, differences were considered statistically significant with $P < 0.05$.

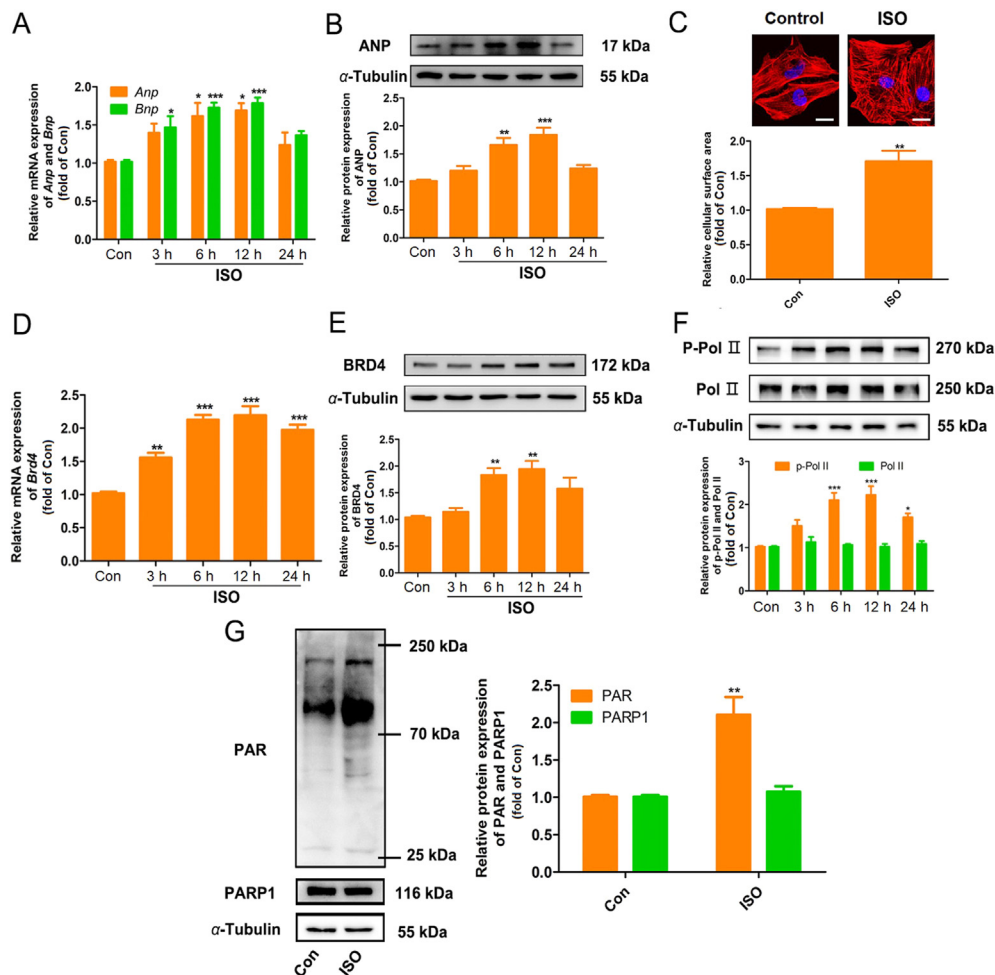


Figure 1 BRD4 expression was upregulated in hypertrophic NRCMs following ISO treatment. Cultured NRCMs were incubated with 10 μ mol/L ISO for the indicated durations. (A) The mRNA levels of *Anp*, *Bnp* were determined by qRT-PCR. (B) The protein expression of ANP was detected by Western blot analysis. (C) Cells were treated with 10 μ mol/L ISO for 12 h. The cell surface area was measured by rhodamine-phalloidin staining. Scale bar = 20 μ m. (D) *Brd4* mRNA expression was determined by qRT-PCR. (E) and (F) Western blot analysis was conducted to detect the protein level of BRD4, total RNA Pol II and phosphorylated RNA Pol II. (G) The total expression PARP1 and PARP1 activity were determined by Western blot. Data are presented as mean \pm SEM, $n = 4$; * $P < 0.05$, ** $P < 0.01$, *** $P < 0.001$ vs. Control group.

3. Results

3.1. *BRD4* expression and *PARP1* activity were increased in ISO-induced cardiac hypertrophy in vitro and in vivo

ISO, a nonselective β -adrenergic receptor (β -AR) agonist, has been widely used to induce cardiac hypertrophy^{24,32}. NRCMs were incubated with 10 μ mol/L ISO for the times indicated. As showed in Fig. 1A and B, ISO treatment for 6 and 12 h significantly elevated the expression of ANP and BNP, which are the markers of cardiac hypertrophy. Cell surface area was increased after stimulation by ISO for 12 h (Fig. 1C). These results indicate that ISO-induced cardiomyocyte hypertrophy model was successfully established. In these hypertrophic cardiomyocytes, the mRNA levels of *Brd2* and *Brd4* were increased while *Brd3* was not significantly changed (Fig. 1D and Supporting Information Fig. S2). Furthermore, ISO induced elevation of BRD4 protein

expression (Fig. 1E). Since gene transcription elongation induced by BRD4 is dependent on the phosphorylation of RNA Pol II, we detected the changes of phosphorylated RNA Pol II in hypertrophic cardiomyocytes. Western blot analysis suggested that Pol II phosphorylation was prominently increased by ISO treatment for 6 and 12 h, although the total protein expression was unaltered (Fig. 1F). The activity of PARP1, as determined by the PARylation level of total proteins, was elevated by ISO treatment without affecting PARP1 protein expression (Fig. 1G).

In vivo, SD rats were submitted to subcutaneous injection of ISO (1.2 mg/kg/day, for 7 days) to stimulate pathological cardiac hypertrophy. In this study, the hearts of ISO-treated rats were obviously larger than those of control animals receiving NS, and revealed typical hypertrophic changes, as showed by gross morphologic examination, HE staining, PSR staining and echocardiographic analysis (Fig. 2A–D). ISO triggered a tendency for increases in left ventricular anterior wall thickness (LVAW), left

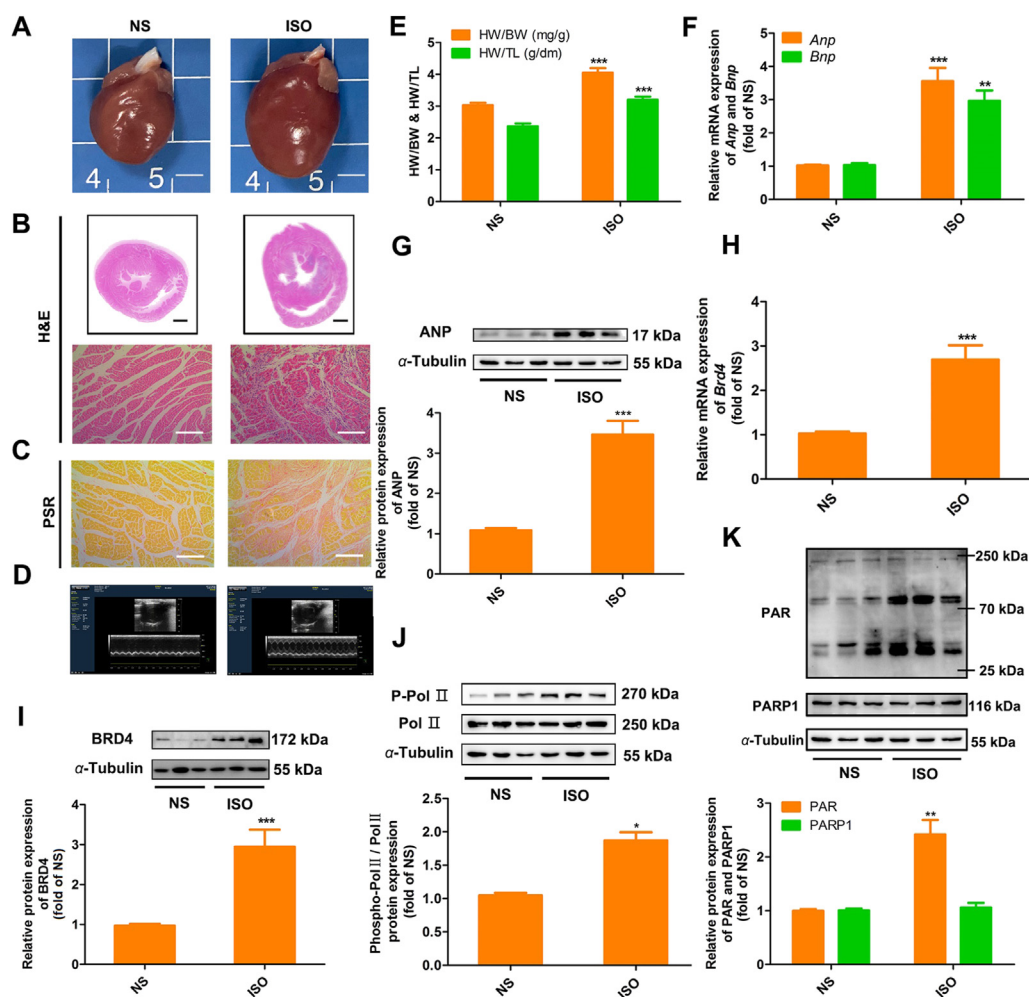


Figure 2 BRD4 expression was upregulated in hypertrophic hearts of SD rats induced by ISO treatment. SD rats were submitted to the s.c. injection of ISO (1.2 mg/kg/day) for 7 days. The control animals obtained normal saline (NS). (A)–(D) Gross hearts, HE-stained and PSR-stained cross sections of the left ventricle, and representative echocardiographic graphs are shown, respectively. Scale bar = 2 mm (A), 50 μ m (B) and (C). (E) The ratios of HW/BW and HW/TL were measured. (F) and (H) The mRNA levels of *Anp*, *Bnp* and *Brd4* were detected by qRT-PCR. (G) and (I) The protein levels of ANP, BNP and BRD4 were determined by Western blot in cardiac tissues. (J) and (K) Western blot analysis was conducted to determine the phosphorylation of RNA Pol II, total expression and activity of PARP1. Data are presented as the mean \pm SEM, $n = 6$; * $P < 0.05$, ** $P < 0.01$, *** $P < 0.001$ vs. NS group.

ventricular posterior wall thickness (LVPW), ejection fraction (EF %) and fractional shortening (FS%), as well as a tendency for reduced left ventricular internal diameter (LVID) (Supporting Information Table S4). The ratios of heart weight (HW)/body weight (BW) and heart weight/tibia length (TL) were also increased in ISO group (Fig. 2E). In addition, the mRNA and protein levels of hypertrophic markers, including ANP and BNP, were remarkably elevated (Fig. 2F and G). The above results suggest the successful induction of cardiac hypertrophy in SD rats by ISO. In the cardiac tissues of these cardiac hypertrophic rats, both mRNA and protein expressions of BRD4 were significantly upregulated (Fig. 2H and I), accompanied with an increased phosphorylation level of RNA Pol II (Fig. 2J). Additionally, the activity of PARP1 was markedly enhanced following ISO treatment (Fig. 2K). Consistent with the *in vitro* observations, these *in vivo* results confirm that BRD4 expression and PARP1 activity are increased in cardiac hypertrophy.

3.2. BRD4 inhibition repressed cardiac hypertrophy *in vitro* and *in vivo*

Since the above findings revealed an upregulation of BRD4 in cardiac hypertrophy, it is hypothesized that inhibition of BRD4 might protect against cardiac hypertrophy. To test the hypothesis, BET inhibitors JQ1 and MS417 were used to treat cardiomyocytes (1 $\mu\text{mol/L}$ for 6 h)^{33–35}. As shown in Fig. 3A and B, both JQ1 and MS417 inhibited ISO-induced elevation of mRNA and protein levels of ANP and BNP. Similarly, knockdown of endogenous

BRD4 by siRNA remarkably attenuated ISO-induced hypertrophic responses, as demonstrated by the expressions of ANP and BNP, as well as the cardiomyocyte surface area (Fig. 3C–E). In the contrary, overexpression of BRD4 by transfection with plasmid encoding BRD4 augmented the cell surface area and expressions of hypertrophic genes (Fig. 4A–C), together with an increased phosphorylation of RNA Pol II (Fig. 4D).

Moreover, AAV-si-BRD4 was introduced into the left ventricles of SD rats through intramyocardial injection. The delivery of AAV-si-BRD4 attenuated ISO-induced hypertrophic response *in vivo*, as demonstrated by gross morphologic examination, HE staining, PSR staining, WGA staining, echocardiography data, the HW/BW and HW/TL ratios, as well as the expression of hypertrophic marker genes (Fig. 5 and Supporting Information Table S5). Furthermore, the expression of BRD4 is associated with the degree of cardiac hypertrophy (Supporting Information Fig. S3). Taken together, these observations suggest that BRD4 overexpression could promote cardiac hypertrophy, whereas BRD4 knockdown or inhibition ameliorates pathological cardiac hypertrophy.

3.3. PARP1 accelerated cardiac hypertrophy

To investigate the involvement of PARP1 in cardiac hypertrophy, PARP1 was inhibited or overexpressed in NRCMs. PARP1 inhibitors 3AB and ABT-888 (10 $\mu\text{mol/L}$ for 24 h) significantly reversed ISO-induced ANP upregulation (Fig. 6A). By contrast, infection of Ad-PARP1 enhanced the protein expression of ANP (Fig. 6B). We also examined the role of PARP1 in cardiac

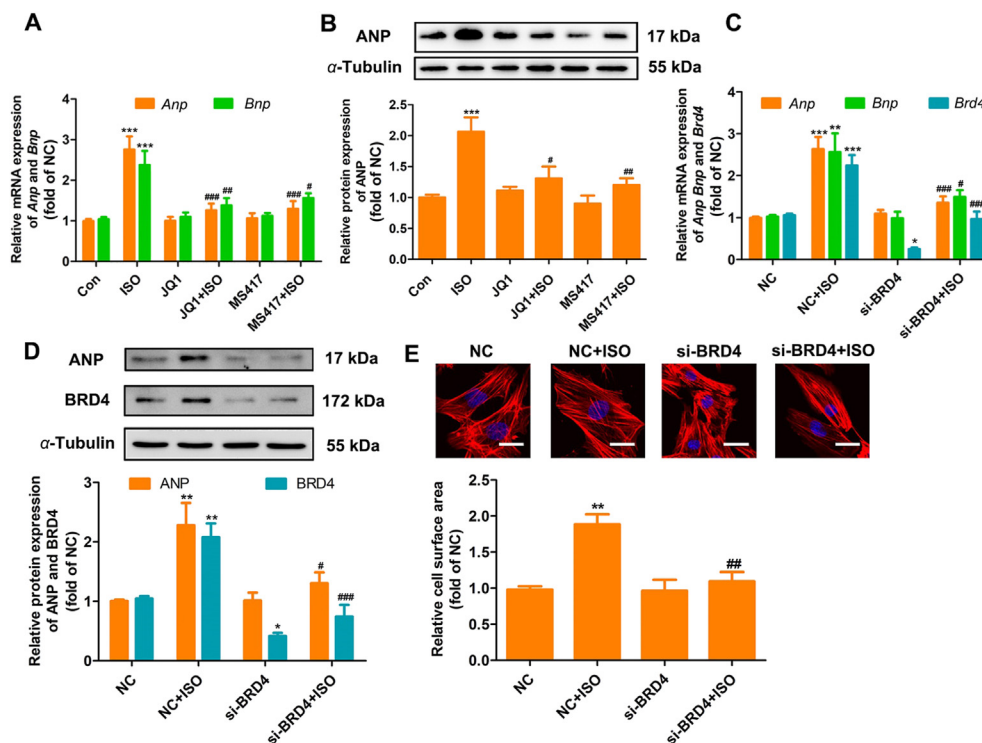


Figure 3 BRD4 inhibitors JQ1 and MS417 or BRD4 knockdown attenuated hypertrophic responses in cardiomyocytes treated with ISO. Cells were treated with BET inhibitors JQ1 and MS417, siRNA targeting *Brd4* (si-BRD4) or negative control (NC) for 48 h, and further incubated with or without 10 $\mu\text{mol/L}$ ISO for 12 h. (A)–(D) The mRNA and protein levels of ANP, BNP, BRD4 were detected by qRT-PCR and Western blot. (E) The cell surface area was measured by rhodamine-phalloidin staining. Scale bar = 20 μm . Data are presented as the mean \pm SEM, $n = 4$; * $P < 0.05$, ** $P < 0.01$, *** $P < 0.001$ vs. Con or NC group; # $P < 0.05$, ### $P < 0.01$, #### $P < 0.001$ vs. ISO or NC+ISO group.

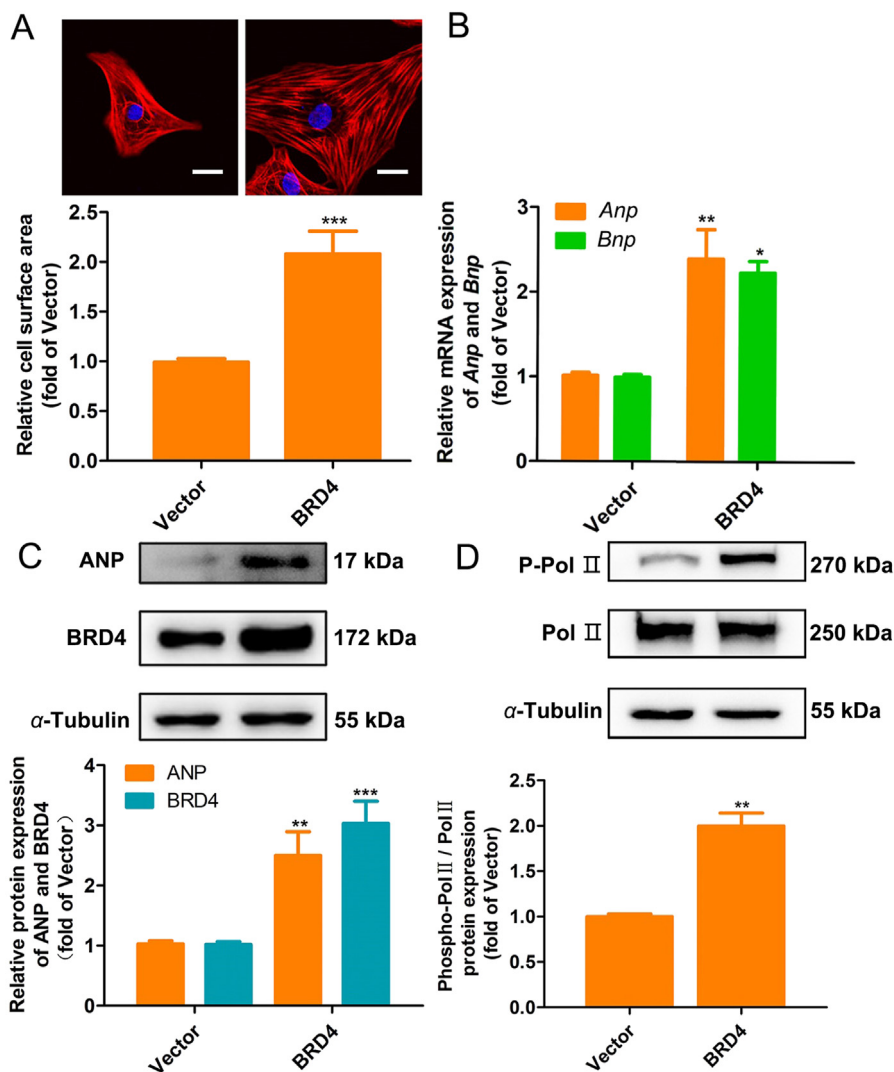


Figure 4 BRD4 overexpression led to hypertrophic responses in NRCMs. Cells were transfected with GV219-BRD4 plasmid or blank vector. (A) The cell surface area was measured by rhodamine-phalloidin staining. Scale bar = 20 μ m. (B) The mRNA levels of *Anp* and *Bnp* were detected by qRT-PCR. (C) BRD4 and ANP protein level was detected by Western blot. (D) The phosphorylation of RNA Pol II was determined by Western blot analysis. Data are presented as the mean \pm SEM, $n = 4$; * $P < 0.05$, ** $P < 0.01$, *** $P < 0.001$ vs. Vector group.

hypertrophy *in vivo*. 3AB was treated in rats (20 mg/kg/day, i.p.) 7 days before ISO injection and continuing for 7 days. As shown in Supporting Information Fig. S4, 3AB ameliorated ISO-induced cardiac hypertrophy *in vivo*. Our results thus confirm that PARP1 accelerated cardiac hypertrophy.

3.4. PARP1 interacted with BRD4 and PARylated BRD4

The colocalization of BRD4 and PARP1 in NRCMs was observed by confocal microscopy (Fig. 7A). As implied by the co-IP data, PARP1 was detected in precipitations pulled down by BRD4 antibody (Fig. 7B), while BRD4 was detected in proteins precipitated by anti-PARP1 consistently (Fig. 7C). These findings provide solid evidence of the interaction between BRD4 and PARP1 in cardiomyocytes. Since the function of PARP1 is mainly dependent on its PARylated activity, we further sought to determine whether BRD4 is PARylated by PARP1 in NRCMs. The PARylation assay results demonstrate that PARylation level of BRD4 was elevated by Ad-PARP1 infection, but was eliminated in

the presence of PARP1 inhibitors 3AB and ABT-888 (Fig. 7D). Moreover, PARP1-mediated PARylation of BRD4 was restrained by transfection with si-PARP1 (Fig. 7E). These observations thus suggest that BRD4 may serve as a substrate of PARP1, and that PARylation of BRD4 is dependent on the activity of PARP1. In ISO-treated cardiomyocytes, interaction between PARP1 and BRD4 was enhanced, accompanied with the increase of BRD4 PARylation (Fig. 7F). Furthermore, PARP1-mediated PARylation of BRD4 was also detected in rat heart tissues. The results show that BRD4 PARylation was increased by ISO treatment but was alleviated by 3AB treatment (Fig. 7G), confirming that BRD4 is PARylated by PARP1 *in vivo*. To further identify the potential PARylated sites of BRD4 by PARP1, we constructed three truncation mutants of BRD4 with HA tag: P1 (1–500 amino acids), P2 (501–699 amino acids) and P3 (700–1400 amino acids), and performed IP assays to test the PARylation levels of these mutants. The results show that only P3 was PARylated, suggesting that the PARylation residue of BRD4 is within 700–1400 amino acids, where contains the CTD domain (Fig. 7H). Taken in conjunction,

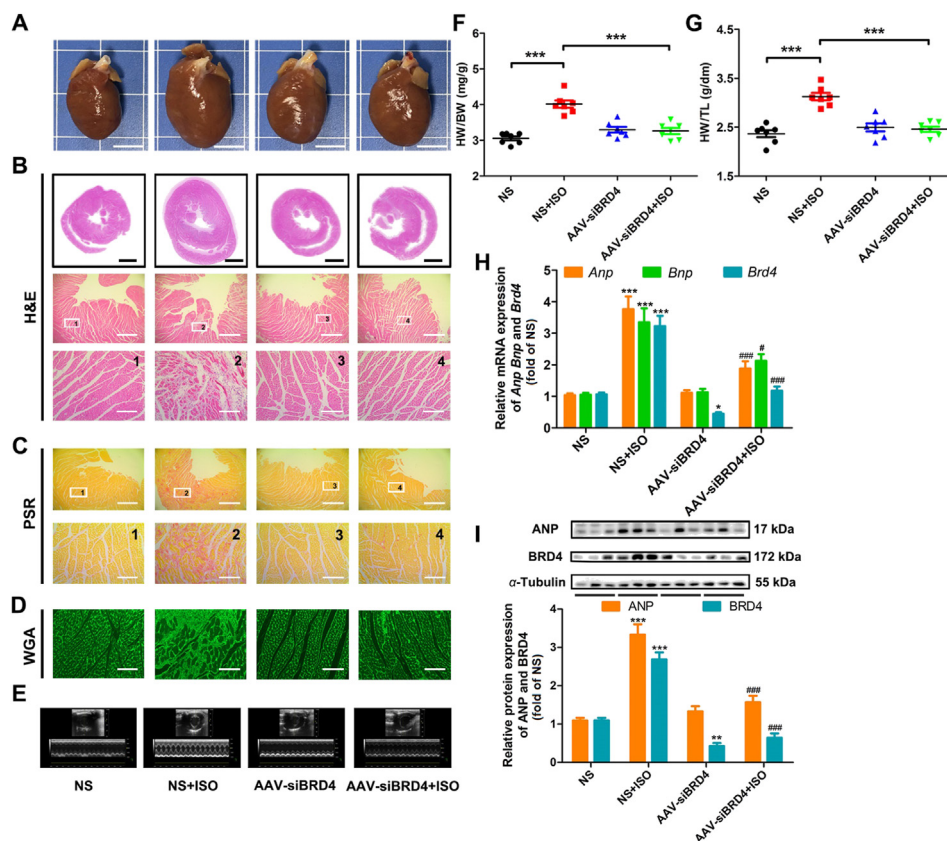


Figure 5 BRD4 knockdown protected SD rats from ISO-induced cardiac hypertrophy. SD rats received intramyocardial injections of adeno-associated virus encoding si-BRD4 (AAV-si-BRD4, 10^{12} particles), the control animals received si-NC (AAV-si-NC, 10^{12} particles), followed by isoprenaline injection (1.2 mg/kg/day, s.c., 7 days) or an equal volume of normal saline (NS). (A)–(E) Hypertrophic changes of the hearts were observed by gross morphologic examination (A), HE staining (B), PSR staining (C), WGA staining (D) and echocardiography (E and Table S4). Scale bar = 50 μ m (B–D). (F) and (G) The HW/BW and HW/TL ratios were calculated. (H) and (I) The mRNA and protein levels of ANP, BNP and BRD4 were measured by qRT-PCR and Western blot. Data are presented as the mean \pm SEM, $n = 7$; * $P < 0.05$, ** $P < 0.01$, *** $P < 0.001$ vs. NS group; # $P < 0.05$, ## $P < 0.01$, ### $P < 0.001$ vs. NS+ISO group.

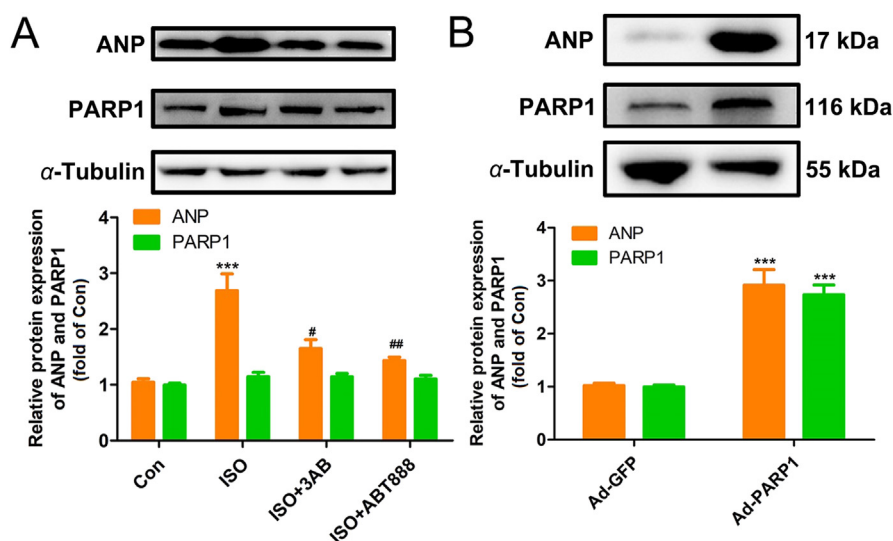


Figure 6 The involvement of PARP1 in cardiac hypertrophy. (A) Cells were incubated with 3AB or ABT888 (10 μ mol/L, 24 h) followed by incubation with ISO (10 μ mol/L, 12 h). The protein level of ANP were determined by Western blot. (B) Cells were infected with PARP1 adenovirus. Western blot analysis was conducted to determine the change of ANP expression. All values are presented as the mean \pm SEM, $n = 4$; * $P < 0.05$, ** $P < 0.01$, *** $P < 0.001$ vs. Con or Ad-GFP group; # $P < 0.05$, ## $P < 0.01$ vs. ISO group.

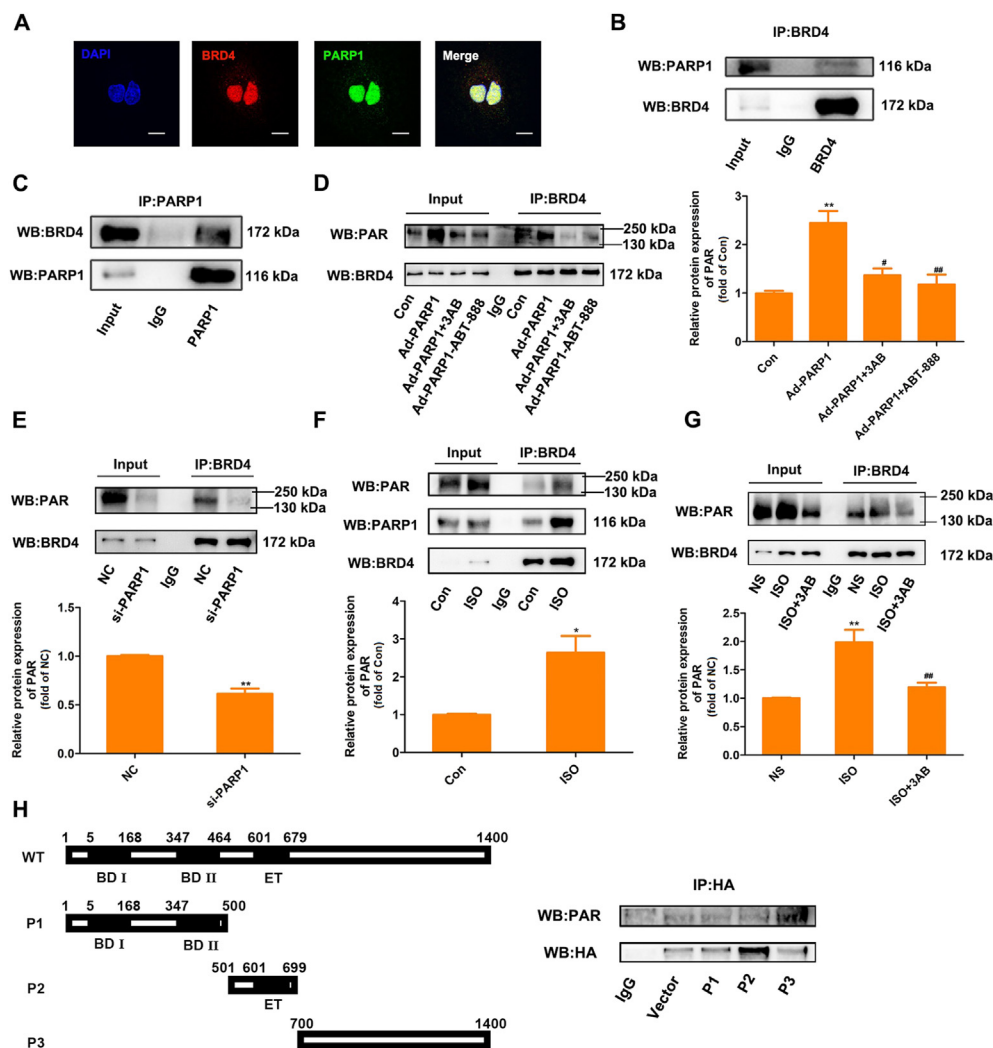


Figure 7 PARP1 interacts and poly(ADP-ribosyl)ates BRD4. (A) The intracellular colocalization of PARP1 and BRD4 was confirmed in NRCMs, by confocal microscopy. (B) NRCMs were transfected with infected with GV219-BRD4 plasmid and were precipitated by anti-BRD4, followed by subjection to co-IP assays. (C) NRCMs were infected with Ad-PARP1 and were precipitated by anti-PARP1 for BRD4 detection in reciprocal co-IP assays. (D) NRCMs were incubated with 3AB or veliparib (ABT-888) followed by Ad-PARP1 infection, immunoprecipitated with anti-BRD4 and subsequently subjected to immunoblotting assays. (E) NRCMs were transfected with si-PARP1 and then immunoprecipitated with anti-BRD4 and subsequently subjected to immunoblotting assays. (F) NRCMs were incubated with ISO and then immunoprecipitated with anti-BRD4 and subsequently subjected to immunoblotting assays. (G) Rat heart tissues, which were treated with 3AB followed by ISO, were immunoprecipitated with anti-BRD4 and subsequently subjected to Western blot analysis. (H) Three large deletion BRD4 mutants (P1, P2 and P3) were detected by immunoprecipitation assays. P1: 1–500 amino acids; P2: 501–699 amino acids; P3: 700–1400 amino acids. Data are presented as the mean \pm SEM, $n = 3$; * $P < 0.05$, ** $P < 0.01$ vs. Control group; # $P < 0.05$, ## $P < 0.01$ vs. Ad-PARP1 group.

these observations indicate that PARP1 interacts with BRD4 and PARylates it at the CTD domain.

3.5. Involvement of BRD4 in PARP1-mediated cardiomyocyte hypertrophy

Since BRD4 acts as a downstream substrate of PARP1, we further explored whether PARylation of BRD4 is involved in the prohypertrophic effects of PARP1. As shown in Fig. 8A and B, inhibition of BRD4 by JQ1 or MS417, or knockdown of BRD4 by siRNA remarkably repressed Ad-PARP1-mediated upregulation of ANP. In the contrary, overexpression of BRD4 abolished the anti-hypertrophic effect of PARP1 inhibitors (Fig. 8C). These rescue experiments support the conclusion that BRD4 is involved in the PARP1-induced cardiac hypertrophy.

3.6. The transcription elongation mediated by BRD4 is promoted by PARP1

BRD4 has previously been shown to be recruited to the TSS of hypertrophic genes^{36,37}. In our study, we verified the binding of BRD4 on ANP and BNP TSS through ChIP-qPCR and used β -actin as a negative control to demonstrate the specificity of BRD4 binding to ANP and BNP promoters (Supporting Information Fig. S5). Based on the above findings, it is hypothesized whether or not this process is affected by PARP1. To test this hypothesis, cultured NRCMs were infected with Ad-PARP1 or treated with ABT-888 after ISO stimulation, followed by ChIP experiments to test the binding capacity of BRD4 to TSS of ANP and BNP (Fig. 9A). As shown in Fig. 9B and C, ISO treatment induced the recruitment of BRD4 at the TSS of ANP and BNP, whereas

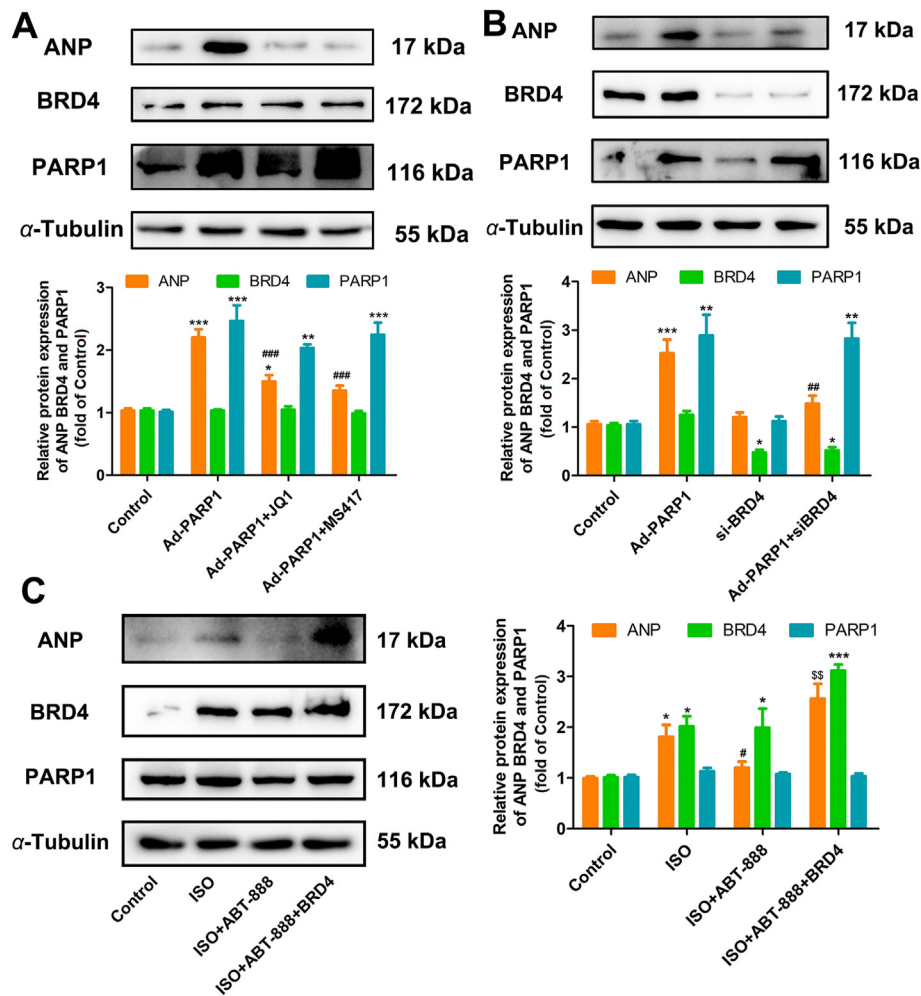


Figure 8 Involvement of BRD4 in PARP1-mediated cardiomyocyte hypertrophy. (A) NRCMs were incubated with 3AB or ABT888 (10 μ mol/L, 24 h) followed by Ad-PARP1 infection. The protein level of ANP was determined by Western blot. (B) Cells were transfected with si-BRD4 followed by BRD4 adenovirus. (C) Cells were incubated with ABT888 (10 μ mol/L, 24 h) followed by ISO treatment and then transfected with BRD4 plasmid. Western blot analysis was conducted to determine the change of ANP expression. All values are presented as the mean \pm SEM, $n = 4$; * $P < 0.05$, ** $P < 0.01$, *** $P < 0.001$ vs. Control group; # $P < 0.05$, ## $P < 0.01$, ### $P < 0.001$ vs. Ad-PARP1 or ISO group; $^{SS}P < 0.01$ vs. ISO+ABT888 group.

PARP1 inhibitor ABT-888 reversed the effect of ISO. In addition, PARP1 overexpression promoted the binding of BRD4 to the TSS of hypertrophic biomarkers (Fig. 9D and E). Moreover, overexpression of PARP1 enhanced the phosphorylation of RNA Pol II, which was inhibited by BRD4 inhibitors JQ1 and MS417 (Fig. 9F). Taken together, these data imply that PARylation of BRD4 by PARP1 might facilitate the binding of BRD4 to the TSS of hypertrophic genes, enhancing the phosphorylation of RNA Pol II, subsequently promoting the transcription of hypertrophic genes and leading to cardiac hypertrophy.

4. Discussion

During pathological cardiac hypertrophy, ANP and BNP, small peptide hormones encoded by the *Nppa* and *Nppb* genes and are some of the most commonly measured members of the fetal gene program³⁸, are secreted in response to cardiac wall pressure. Therefore, they are regarded as typical biomarkers of cardiac hypertrophy and heart failure^{38,39}.

Epigenetic readers have attracted increasing attention following the discovery that they are pivotal in the pathogenesis of numerous diseases. Being one of the most attractive epigenetic readers, the BET family is capable to bind to the acetyl-lysine residues in histones, thus regulating transcription program^{36,37}. Evidences indicated that inhibitors of BET family protect against cardiac diseases such as heart failure, cardiac hypertrophy and acute myocardial infarction, suggest the potential of BET family proteins as promising therapeutic targets^{16,40–42}. Among all these BET family proteins, BRD4 has been shown to be involved in pathological cardiac hypertrophy^{19,20,43}. In line with these findings, the present study confirms that BRD4 plays a crucial role in ISO-induced cardiac hypertrophy. The mRNA and protein expressions of BRD4 were increased in ISO-induced cardiac hypertrophy *in vivo* and *in vitro* (Figs. 1D, E, 2H and I). Inhibition or knockdown of BRD4 prevented ISO-induced hypertrophic responses (Figs. 3, 5 and Fig. S3), whereas overexpression of BRD4 promoted the development of cardiomyocyte hypertrophy (Fig. 4). These evidences indicate that BRD4 could be used as a biomarker of cardiac hypertrophy. Future studies in hearts of *Brd4*^{-/-} mice

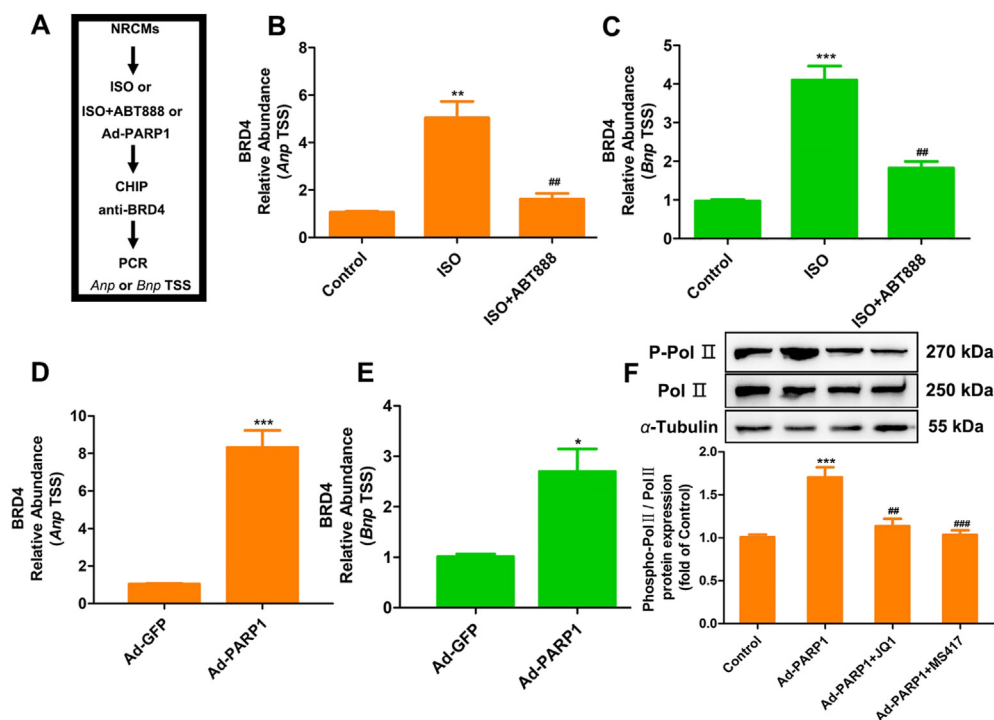


Figure 9 The transcription elongation mediated by BRD4 is promoted by PARP1. (A) NRCMs were infected with Ad-PARP1 or treated with ABT-888 after stimulation with ISO. (B)–(E) Chromatin immunoprecipitation (ChIP) was performed with a BRD4-specific antibody and qPCR was conducted to determine the change of BRD4 abundance at ANP and BNP TSSs. (F) NRCMs were incubated with 3AB or ABT888 (10 μ mol/L, 24 h) followed by Ad-PARP1 infection. The phosphorylation of RNA Pol II was determined by Western blot. Data are presented as the mean \pm SEM, $n = 4$; * $P < 0.05$, ** $P < 0.01$, *** $P < 0.001$ vs. Control or Ad-GFP group; # $P < 0.05$, ## $P < 0.01$, ### $P < 0.001$ vs. ISO or Ad-PARP1 group.

will be conducted to provide a more solid support to our conclusions that BRD4 plays a pivotal role in cardiac hypertrophy.

The most intriguing finding of this study is that there exists cross-interaction between BRD4 and PARP1. PARP1 is the most abundant one among the 18 PARP isoforms, and accounts for more than 90% of the catalytic activity of PARP^{44–46}. Excessive activation of PARP1 has been observed in the development of various cardiovascular diseases, including atherosclerosis, acute myocardial infarction/reperfusion injury and congestive heart failure^{22,23}. Indeed, this study shows that PARP1 activity was increased in ISO-induced cardiac hypertrophy *in vivo* and *in vitro* (Figs. 1G and 2K). Additionally, PARP1 overexpression induced cardiomyocyte hypertrophy, while PARP1 inhibitors 3AB and ABT-888 reversed ISO-induced upregulation of hypertrophic genes (Fig. 6). These observations are consistent with previous results in our laboratory^{24–26}, suggesting that activation of PARP1 contributes to the development of cardiac hypertrophy. Interestingly, BRD4 is involved in PARP1-induced cardiac hypertrophy, as implied by the observations that BRD4 inhibition or silencing reversed PARP1-induced hypertrophic responses, and that BRD4 overexpression suppressed the anti-hypertrophic effect of PARP1 inhibitors (Fig. 8). These findings shed new lights on the mechanism of PARP1-induced cardiac hypertrophy *via* BRD4.

BRD4 has physical interaction with PARP1 and undergoes PARylation by PARP1. This conclusion is supported by results of IF, co-IP and PARylation assays (Fig. 7). The PARylation of BRD4 was augmented by PARP1 overexpression, but was reversed by PARP1 inhibitors, which was also restrained by

PARP1 knockdown in cardiomyocytes (Fig. 7D and E). In addition, the interaction of BRD4 and PARP1, and PARylation of BRD4, were enhanced when PARP1 activity was increased in ISO-treated cardiomyocytes and heart tissues of SD rats, whereas were alleviated by 3AB treatment (Fig. 7F and G). These results suggest that PARylation of BRD4 is dependent on the activity of PARP1, and that BRD4 is a substrate protein of PARP1. However, the present study did not support that PARP1 PARylates the other BET family members like BRD2, even though the mRNA levels of *Brd2* and *Brd4* were both increased by ISO treatment (Fig. S2), which implies that BRD2 might also participate in the development of cardiac hypertrophy. This conclusion is supported by the co-IP results that PARP1 did not interact with BRD2 (Supporting Information Fig. S6).

We further investigated the PARylation modification sites of BRD4. During PARylation modification, ADP-riboses are transferred to the substrates. However, the number of transferred ADP-riboses is hard to determine, which brings difficulties for identifying the modification sites. To determine the modification sites of BRD4, we constructed three truncation mutants of BRD4 according to the domains of BRD4. BRD4 contains three kinds of domains, including two tandem bromodomains (BD I and BD II), an ET domain and a CTD region. The bromodomains are required for epigenetic regulation of gene transcription through interaction with nucleosomes within chromatin⁴⁷. The ET domain is a conserved region that fulfills its regulatory function by recruiting specific effector proteins⁴⁸. The CTD interacts with the positive transcription elongation factor b (P-TEFb), a complex containing

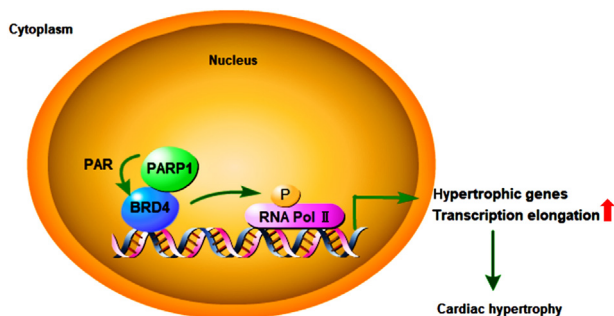


Figure 10 Scheme of this study. In response to hypertrophic stimulus, BRD4 was PARylated by PARP1 which promoted the recruitment of BRD4 at the TSS of hypertrophic genes, enhancing the phosphorylation of RNA pol II, thereby promoting the transcription of hypertrophic genes, ultimately inducing cardiac hypertrophy.

CDK9 and cyclin T, which is able to phosphorylates serine residues of the RNA Pol II C-terminal motif (CTM)⁴⁹. Our data show that P3 truncation of BRD4, which mainly contains CTD, was PARylated by PARP1 (Fig. 7H). It thus suggests that the PARylation modification sites of BRD4 locate at CTD region. Since PARylation usually takes place on Asp(D), Glu(E) and Lys(K), and several PARylation motifs (PXE, EP, and EXXG) have been identified^{50–52}, six motifs within the CTD region are predicted to be the potential PARylation sites (Supporting Information Fig. S7). Future studies will be conducted to explore the exact PARylation sites of BRD4 targeted by PARP1.

Taken into considerations that CTD region of BRD4 was PARylated by PARP1, it is probable that the function of CTD in BRD4 might be altered. The CTD of BRD4 is responsible for the recruitment of P-TEFb complex to TSS of target genes. BRD4 promotes the activation of P-TEFb from its negative regulators 7SK RNA and HEXIM1 protein, facilitating Ser2 phosphorylation in RNA Pol II, leading to the binding of Pol II to chromatin, finally promoting transcription elongation⁵³. Indeed, the binding of BRD4 to TSS of hypertrophic genes and the phosphorylation of RNA Pol II are promoted by BRD4 PARylation. This is implied by the following observations: (1) PARP1 inhibition impaired the binding of BRD4 to TSS of ANP and BNP; (2) PARP1 overexpression facilitated the recruitment of BRD4 to TSS of the hypertrophic genes; and (3) the phosphorylation of RNA pol II was enhanced by PARP1 overexpression, but was reversed by BRD4 inhibitors (Fig. 9). It is still unclear how PARylation of BRD4 facilitates its recruitment at TSS of hypertrophic biomarkers. It is speculated that PARylation of BRD4 might lead to a change of its structure, and provides a stable structure conformation for the binding of P-TEFb complex and the hyperacetylated chromatin.

5. Conclusions

The present study identifies PARylation as a novel post-translational modification of BRD4 mediated by PARP1 that participates in ISO-induced cardiac hypertrophy. PARylation of BRD4 at the CTD domain facilitates its recruitment at the TSS of hypertrophic genes, enhancing the phosphorylation of RNA pol II, thereby promoting the transcription of hypertrophic genes, ultimately inducing cardiac hypertrophy (Fig. 10). Strategies targeting inhibition of PARP1-BRD4

might suggest therapeutic potential for pathological cardiac hypertrophy.

Acknowledgments

This work was supported by grants from the National Natural Science Foundation of China (81872860, 81673433, and 81973318), Local Innovative and Research Teams Project of Guangdong Pearl River Talents Program (2017BT01Y093, China), National Major Special Projects for the Creation and Manufacture of New Drugs (2019ZX09301104, China), Special Program for Applied Science and Technology of Guangdong Province (2015B020232009, China), National Engineering and Technology Research Center for New drug Druggability Evaluation (Seed Program of Guangdong Province, 2017B090903004, China), Guangdong Basic and Applied Basic Research Foundation (2019A1515011256, China), Guangzhou Science and Technology Program Project (201604020121 and 201804010227, China), Yang Fan Project of Guangdong Province (Grant No. 2014YT02S044, China), and Guangdong Provincial Key Laboratory of Construction Foundation (No. 2017B030314030, China).

Author contributions

Zhenzhen Li, Zhuoming Li and Peiqing Liu designed and conducted the study, analyzed the data, and prepared the manuscript. Zhen Guo and Rui Lan performed the animal experiments. Sidong Cai, Zhirong Lin and Junjian Wang collected and interpreted the data. Zhenzhen Li and Jingyan Li revised the manuscript.

Conflicts of interest

The authors declare no conflict of interests.

Appendix A. Supporting information

Supporting data to this article can be found online at <https://doi.org/10.1016/j.apsb.2020.12.012>.

References

1. Yan K, Wang K, Li P. The role of post-translational modifications in cardiac hypertrophy. *J Cell Mol Med* 2019;**23**: 3795–807.
2. Balakumar P, Jagadeesh G. Multifarious molecular signaling cascades of cardiac hypertrophy: can the muddy waters be cleared?. *Pharmacol Res* 2010;**62**:365–83.
3. Adzika GK, Machuki JO, Shang W, Hou H, Ma T, Wu L, et al. Pathological cardiac hypertrophy: the synergy of adenylyl cyclases inhibition in cardiac and immune cells during chronic catecholamine stress. *J Mol Med* 2019;**97**:897–907.
4. Barnes CE, English DM, Cowley SM. Acetylation & Co: an expanding repertoire of histone acylations regulates chromatin and transcription. *Essays Biochem* 2019;**63**:97–107.
5. Greco CM, Condorelli G. Epigenetic modifications and noncoding RNAs in cardiac hypertrophy and failure. *Nat Rev Cardiol* 2015;**12**: 488–97.
6. Chen D, Shen A, Fang G, Liu H, Zhang M, Tang S, et al. Tetrahydroisoquinolines as novel histone deacetylase inhibitors for treatment of cancer. *Acta Pharm Sin B* 2016;**6**:93–9.

7. Choudhary C, Weinert BT, Nishida Y, Verdin E, Mann M. The growing landscape of lysine acetylation links metabolism and cell signalling. *Nat Rev Mol Cell Biol* 2014;**15**:536–50.
8. Bagchi RA, Weeks KL. Histone deacetylases in cardiovascular and metabolic diseases. *J Mol Cell Cardiol* 2019;**130**:151–9.
9. Olson EN, Backs J, McKinsey TA. Control of cardiac hypertrophy and heart failure by histone acetylation/deacetylation. *Novartis Found Symp* 2006;**274**:3–12.
10. Li J, Huang J, Lu J, Guo Z, Li Z, Gao H, et al. Sirtuin 1 represses PKC-zeta activity through regulating interplay of acetylation and phosphorylation in cardiac hypertrophy. *Br J Pharmacol* 2019;**176**:416–35.
11. Peng C, Luo X, Li S, Sun H. Phenylephrine-induced cardiac hypertrophy is attenuated by a histone acetylase inhibitor anacardic acid in mice. *Mol Biosyst* 2017;**13**:714–24.
12. Ntranos A, Casaccia P. Bromodomains: translating the words of lysine acetylation into myelin injury and repair. *Neurosci Lett* 2016;**625**:4–10.
13. Taniguchi Y. The bromodomain and extra-terminal domain (BET) family: functional anatomy of BET paralogous proteins. *Int J Mol Sci* 2016;**17**:1849.
14. Zhang B, Lyu J, Yang EJ, Liu Y, Wu C, Pardeshi L, et al. Class I histone deacetylase inhibition is synthetic lethal with BRCA1 deficiency in breast cancer cells. *Acta Pharm Sin B* 2020;**10**:615–27.
15. Wang CY, Filippakopoulos P. Beating the odds: BETs in disease. *Trends Biochem Sci* 2015;**40**:468–79.
16. Duan Q, McMahon S, Anand P, Shah H, Thomas S, Salunga HT, et al. BET bromodomain inhibition suppresses innate inflammatory and profibrotic transcriptional networks in heart failure. *Sci Transl Med* 2017;**9**:eaah5084.
17. Cully M. Cardiovascular disease: BET inhibitor attenuates heart failure. *Nat Rev Discov* 2017;**16**:453.
18. Haldar SM, McKinsey TA. BET-tuning on chromatin-based therapeutics for heart failure. *J Mol Cell Cardiol* 2014;**74**:98–102.
19. Spiltoir JI, Stratton MS, Cavasin MA, Demos-Davies K, Reid BG, Qi J, et al. BET acetyl-lysine binding proteins control pathological cardiac hypertrophy. *J Mol Cell Cardiol* 2013;**63**:175–9.
20. Stratton MS, Lin CY, Anand P, Tatman PD, Ferguson BS, Wickers ST, et al. Signal-dependent recruitment of BRD4 to cardiomyocyte super-enhancers is suppressed by a microRNA. *Cell Rep* 2016;**16**:1366–78.
21. Scobie KN, Damez-Werno D, Sun H, Shao N, Gancarz A, Panganiban CH, et al. Essential role of poly(ADP-ribosylation) in cocaine action. *Proc Natl Acad Sci U S A* 2014;**111**:2005–10.
22. Henning RJ, Bourgeois M, Harbison RD. Poly(ADP-ribose) polymerase (PARP) and PARP inhibitors: mechanisms of action and role in cardiovascular disorders. *Cardiovasc Toxicol* 2018;**18**:493–506.
23. Lu J, Li J, Hu Y, Guo Z, Sun D, Wang P, et al. Chrysophanol protects against doxorubicin-induced cardiotoxicity by suppressing cellular PARylation. *Acta Pharm Sin B* 2019;**9**:782–93.
24. Lu J, Zhang R, Hong H, Yang Z, Sun D, Sun S, et al. The poly(ADP-ribosylation) of FoxO3 mediated by PARP1 participates in isoproterenol-induced cardiac hypertrophy. *Biochim Biophys Acta* 2016;**1863**:3027–39.
25. Wang L, Li Z, Tan Y, Li Q, Yang H, Wang P, et al. PARP1 interacts with STAT3 and retains active phosphorylated-STAT3 in nucleus during pathological myocardial hypertrophy. *Mol Cell Endocrinol* 2018;**474**:137–50.
26. Feng GS, Zhu CG, Li ZM, Wang PX, Huang Y, Liu M, et al. Synthesis of the novel PARP-1 inhibitor AG-690/11026014 and its protective effects on angiotensin II-induced mouse cardiac remodeling. *Acta Pharmacol Sin* 2017;**38**:638–50.
27. Li Q, Li ZM, Sun SY, Wang LP, Wang PX, Guo Z, et al. PARP1 interacts with HMGB1 and promotes its nuclear export in pathological myocardial hypertrophy. *Acta Pharmacol Sin* 2019;**40**:589–98.
28. Yu SS, Cai Y, Ye JT, Pi RB, Chen SR, Liu PQ, et al. Sirtuin 6 protects cardiomyocytes from hypertrophy *in vitro* via inhibition of NF-kappaB-dependent transcriptional activity. *Br J Pharmacol* 2013;**168**:117–28.
29. Zhou SG, Zhou SF, Huang HQ, Chen JW, Huang M, Liu PQ. Proteomic analysis of hypertrophied myocardial protein patterns in renally hypertensive and spontaneously hypertensive rats. *J Proteome Res* 2006;**5**:2901–8.
30. Li Z, Zhang X, Guo Z, Zhong Y, Wang P, Li J, et al. SIRT6 suppresses NFATc4 expression and activation in cardiomyocyte hypertrophy. *Front Pharmacol* 2018;**9**:1519.
31. Curtis MJ, Alexander S, Cirino G, Docherty JR, George CH, Giembycz MA, et al. Experimental design and analysis and their reporting II: updated and simplified guidance for authors and peer reviewers. *Br J Pharmacol* 2018;**175**:987–93.
32. Guo Z, Lu J, Li J, Wang P, Li Z, Zhong Y, et al. JMJD3 inhibition protects against isoproterenol-induced cardiac hypertrophy by suppressing beta-MHC expression. *Mol Cell Endocrinol* 2018;**477**:1–14.
33. Huang W, Zheng X, Yang Y, Wang X, Shen Z. An overview on small molecule inhibitors of BRD4. *Mini Rev Med Chem* 2016;**16**:1403–14.
34. Duan Y, Guan Y, Qin W, Zhai X, Yu B, Liu H. Targeting Brd4 for cancer therapy: inhibitors and degraders. *MedChemComm* 2018;**9**:1779–802.
35. Sun C, Yin J, Fang Y, Chen J, Jeong KJ, Chen X, et al. BRD4 inhibition is synthetic lethal with PARP inhibitors through the induction of homologous recombination deficiency. *Cancer Cell* 2018;**33**:401–416.e8.
36. Cochran AG, Conery AR, Sims 3rd RJ. Bromodomains: a new target class for drug development. *Nat Rev Drug Discov* 2019;**18**:609–28.
37. Alqahtani A, Choucair K, Ashraf M, Hammouda DM, Alloghbi A, Khan T, et al. Bromodomain and extra-terminal motif inhibitors: a review of preclinical and clinical advances in cancer therapy. *Future Sci OA* 2019;**5**:Fso372.
38. Cox EJ, Marsh SA. A systematic review of fetal genes as biomarkers of cardiac hypertrophy in rodent models of diabetes. *PLoS One* 2014;**9**:e92903.
39. Dietz JR. Mechanisms of atrial natriuretic peptide secretion from the atrium. *Cardiovasc Res* 2005;**68**:8–17.
40. Liu CF, Tang WHW. Epigenetics in cardiac hypertrophy and heart failure. *JACC Basic Transl Sci* 2019;**4**:976–93.
41. Ummarino D. Heart failure: BRD4 inhibition slows HF progression. *Nat Rev Cardiol* 2017;**14**:382–3.
42. Sun Y, Huang J, Song K. BET protein inhibition mitigates acute myocardial infarction damage in rats via the TLR4/TRAF6/NF-kappaB pathway. *Exp Ther Med* 2015;**10**:2319–24.
43. Chelladurai P, Boucherat O, Stenmark K, Kracht M, Seeger W, Bauer UM, et al. Targeting histone acetylation in pulmonary hypertension and right ventricular hypertrophy. *Br J Pharmacol* 2021;**178**:54–71.
44. Xu S, Bai P, Little PJ, Liu P. Poly(ADP-ribose) polymerase 1 (PARP1) in atherosclerosis: from molecular mechanisms to therapeutic implications. *Med Res Rev* 2014;**34**:644–75.
45. Ame JC, Spenlehauer C, de Murcia G. The PARP superfamily. *Bioessays* 2004;**26**:882–93.
46. Abdelfatah S, Berg A, Huang Q, Yang LJ, Hamdoun S, Klinger A, et al. MCC1019, a selective inhibitor of the Polo-box domain of Polo-like kinase 1 as novel, potent anticancer candidate. *Acta Pharm Sin B* 2019;**9**:1021–34.
47. Jang MK, Mochizuki K, Zhou M, Jeong HS, Brady JN, Ozato K. The bromodomain protein Brd4 is a positive regulatory component of P-TEFb and stimulates RNA polymerase II-dependent transcription. *Mol Cell* 2005;**19**:523–34.
48. Rahman S, Sowa ME, Ottinger M, Smith JA, Shi Y, Harper JW, et al. The Brd4 extraterminal domain confers transcription activation independent of pTEFb by recruiting multiple proteins, including NSD3. *Mol Cell Biol* 2011;**31**:2641–52.
49. Bisgrove DA, Mahmoudi T, Henklein P, Verdin E. Conserved P-TEFb-interacting domain of BRD4 inhibits HIV transcription. *Proc Natl Acad Sci U S A* 2007;**104**:13690–5.

50. Alemasova EE, Lavrik OI. Poly(ADP-ribosylation) by PARP1: reaction mechanism and regulatory proteins. *Nucleic Acids Res* 2019;**47**: 3811–27.
51. Zhang Y, Wang J, Ding M, Yu Y. Site-specific characterization of the Asp- and Glu-ADP-ribosylated proteome. *Nat Methods* 2013;**10**: 981–4.
52. Rouleau M, Aubin RA, Poirier GG. Poly(ADP-ribosyl)ated chromatin domains: access granted. *J Cell Sci* 2004;**117**:815–25.
53. Devaiah BN, Lewis BA, Cherman N, Hewitt MC, Albrecht BK, Robey PG, et al. BRD4 is an atypical kinase that phosphorylates serine2 of the RNA polymerase II carboxy-terminal domain. *Proc Natl Acad Sci U S A* 2012;**109**:6927–32.